

# Achieving Real-Time Target Tracking Using Wireless Sensor Networks

Tian He<sup>§</sup>, Pascal Vicaire<sup>†</sup>, Ting Yan<sup>†</sup>, Liqian Luo\*, Lin Gu<sup>†</sup>, Gang Zhou<sup>†</sup>,  
Radu Stoleru<sup>†</sup>, Qing Cao\*, John A. Stankovic<sup>†</sup> and Tarek Abdelzaher\*

<sup>†</sup>Department of Computer Science, University of Virginia

<sup>§</sup>Department of Computer Science and Engineering, University of Minnesota

## Abstract

*Target tracking systems, consisting of thousands of low-cost sensor nodes, have been used in many application domains such as battlefield surveillance, wildlife monitoring and border security. These applications need to meet certain real-time constraints in response to transient events, such as fast-moving targets. While the real-time performance is a major concern in these applications, it should be compatible with other important system properties such as energy consumption and accuracy. Hence, it is desirable to have the ability to exploit the tradeoffs among them. This work presents the real-time design and analysis of VigilNet, a large-scale sensor network system which tracks, detects and classifies targets in a timely and energy efficient manner. Based on a deadline partition method and theoretical derivations of each sub-deadline, we are able to make guided engineering decisions to meet the end-to-end tracking deadline. To confirm our design and obtain an empirical understanding of these tradeoffs, we invest significant efforts to perform large-scale simulations with 10,000 nodes as well as a field test with 200 XSM motes, running VigilNet. The results from both analysis and evaluation can serve as general design guidelines to build similar real-time systems.*

## 1 Introduction

Recent developments in sensor techniques make wireless sensor networks (WSNs) available to many application domains [6, 12, 17, 26, 32]. Most of these applications, such as battlefield surveillance, disaster and emergency response, deal with various kinds of real-time constraints in response to the physical world. For example, surveillance may require a sensor node to detect and classify a fast moving target within 1 second before it moves out of the sensing range. Compared with the traditional distributed systems, the real-time guarantee for sensor networks is more challenging due to the following reasons. First, sen-

sor networks directly interact with the real world, in which the physical events may exhibit unpredictable *spatiotemporal* properties. These properties are hard to characterize with the traditional methods. Second, although the real-time performance is a key concern, it should be performance compatible with many other critical issues such as energy efficiency and system robustness. For example, it is not efficient to activate the sensors all the time only for the benefit of a fast response. This naive approach severely reduces the system lifetime [12]. Third, the resource constraints restrict the design space we could trade off. For example, the limited computation power in sensor nodes makes the Fast Fourier Transformation not quite suitable for real-time detection. All these issues challenge us with two questions. *How to make the design of a large-scale real-time sensor network system manageable? And how to trade off among system metrics while maintaining the real-time guarantee?* Our answer to these questions, presented in this paper, is a case study of the VigilNet system, a real-time outdoor tracking system using a large-scale wireless sensor network.

Our contribution lies in the following aspects: 1) This work addresses a real-world application with a running real-time system, designed and implemented over last few years. 2) We investigate multi-dimensional tradeoffs between the real-time performance and other system properties. Such investigation provides the guidance for the future development of similar systems. 3) The real-time design and tradeoffs are validated by a large-scale field evaluation with 200 XSM motes and an extensive simulation with 10,000 nodes. These evaluations reveal quite a few practical design suggestions that can be applied to other real-time sensor systems.

The remainder of the paper is organized as follows: Section 2 introduces the tracking process in VigilNet. Section 3 identifies the real-time requirements. Section 4 provides a real-time analysis of VigilNet's tracking performance and its tradeoffs. In Section 5, we evaluate the real-time performance of VigilNet in an outdoor field test. In Section 6, we conduct a large-scale simulation to further validate and analyze the real-time issues in VigilNet. Section 7 discusses the related work. Section 8 concludes the paper.

\*Liqian Luo, Qing Cao and Tarek Abdelzaher are now with University of Illinois, Urbana-Champaign

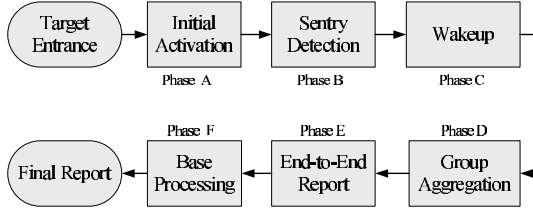


Figure 1: The Delay Breakdown in Tracking Operation

## 2 Overview of VigilNet Tracking Operations

VigilNet is an energy-efficient surveillance and tracking system, designed for spontaneous military operations in remote areas. In these areas, the events of interest happen at a relatively low rate, i.e. the duration of significant events (e.g., intruders) is very short, compared with the overall system lifetime (e.g., 5-minute tracking per day). According to our empirical results [13], nearly 99% of energy is consumed during the idle-waiting period for potential targets. Therefore to conserve energy, the most effective approach is to selectively turn a subset of nodes off, and wake them up on demand in the presence of significant events. This power management technique fundamentally shapes the VigilNet tracking process. It introduces a set of new delays that traditional tracking systems do not experience.

In this section, we give a brief overview of the VigilNet tracking operation, serving as a background for the real-time design and analysis in the following sections. As shown in Figure 1, after a target enters the area, it activates the first sensor node that can confirm the detection, then other nodes nearby are waken up to form a group to deliver the aggregated reports to the base. More specifically, the VigilNet tracking operation has six phases:

- A. Initial Activation:** VigilNet stays in the power management state when there are no targets. The power management protocol puts nodes into either one of two states: *sentry* and *non-sentry*. In brief, a node becomes a sentry node if it is a part of the routing infrastructure or it needs to provide the sensing coverage. Otherwise, it becomes an inactive non-sentry node. The details of sentry selection can be found in [12]. If the sentry nodes are active 100% of time (i.e. the deployed area is always covered), any incoming target is covered by at least one sentry node immediately. On the other hand, if the sentry nodes have a certain duty cycle (i.e. they go to sleep and wake up periodically to save energy), there will be an initial activation delay, denoted as  $T_{initial}$ , before the first sentry node starts to sense the incoming target.
- B. Initial Target Detection:** After the initial activation, it takes a certain delay, defined as  $T_{detection}$ , for the first sentry node to *confirm* the detection. This delay consists of the hardware response delay, the discrete sampling delay and the delay to accumulate a sufficient number of samples before a detection algorithm recognizes the target.

- C. Wake-up:** Normally, the detection from a single sentry node does not provide sufficient confidence in detection and classification, therefore a group-based tracking is designed in VigilNet. In order to form a group with a reasonable size, non-sentry nodes need to be waken up after the initial target detection by a sentry node in Phase B. We define the wake-up delay  $T_{wakeup}$  as the time required for a sentry node to wake up other sleeping non-sentry nodes. This delay is determined by the time to broadcast the wake-up messages.

- D. Group Aggregation:** Once awoken, all nodes that detect the same target join the same logic group to establish a unique one-to-one mapping between this logic group and the detected target. Each group is represented by a leader to maintain the identity of the group as the target moves through the area. Group members (who by definition can sense the target) periodically report to the group leader. A leader starts to report detection to the base after the number of member reports exceeds a certain threshold, defined as the degree of aggregation (DOA). We use  $T_{aggregation}$  to denote the group aggregation delay, which is the time required to collect and process the detection reports from the member nodes.

- E. End-to-End Report:** After the group aggregation, the leader node reports the event to the nearest base. Multiple bases are used to partition a network into several sections, in order to bound the end-to-end delivery delay  $T_{e2e}$ .

- F. Base Processing ( $T_{base}$ ):** A base is in charge of processing the reports from the leaders of different logic groups. Since the reports from the same logic group are spatiotemporal correlated, a string of consecutive reports can be further analyzed and summarized for end users. For example, taking the time stamps and the locations of targets as the inputs, a base uses the least-square estimation to obtain the velocity of each target.

## 3 Real-Time Requirement in VigilNet

To ensure the effectiveness of the target tracking, VigilNet must meet a certain real-time constraint. Specifically, VigilNet should detect, classify and analyze the incoming targets within a certain end-to-end deadline (e.g., 5 seconds from Phase A to F). As shown in Section 2, this deadline involves complex analysis of the whole tracking process. It is not scalable for us to identify a system-wide feasible region within such a high-dimensional design space. Therefore, we adopt the deadline partition method to divide the end-to-end deadline into multiple sub-deadlines. The sub-deadline partition varies with the system configurations. As a concrete example, supposing a target enters the field with a speed up to 20 mph, to guarantee that this target can be detected by the first sentry node with a probability higher than 90%, we need to design a detection algorithm with a sub-deadline less than 1 second, assuming the detection range is 10 meters.

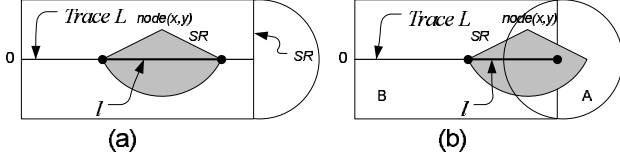


Figure 2: Detection Probability

By confining the real-time decisions within each phase, we make the end-to-end analysis manageable in a lower-dimensional design space. As long as the individual sub-deadlines are met, we have a certain guarantee on the end-to-end delay. To achieve this, we present a set of real-time designs in next section.

## 4 VigilNet Real-Time Tracking Analysis

The description of this section follows the natural order of VigilNet's tracking operations presented in Section 2. Such design and analysis is validated later with a real system implementation consisting of 200 XSM nodes as well as a large-scale simulation in Section 5 and Sections 6, respectively.

### 4.1 Initial Activation Delay and Its Tradeoffs

In a duty-cycle-based power management scheme, the sentry nodes go to sleep and wake up periodically. In this case, the initial activation delay  $T_{initial}$  may not be zero, because sentry nodes near the target's entry point may be asleep when the target enters the field. In this section, we identify a quantitative relationship between the energy savings and the  $T_{initial}$ , which helps us make decisions to guarantee that the initial activation finishes within a given sub-deadline  $D_{initial}$ .

In our VigilNet design, all sentry nodes agree on a common sentry toggle period  $P$  and a common sentry duty cycle  $SDC$ . For each period, a sentry wakes up randomly and stays awake for  $P \cdot SDC$ , then goes to sleep. Assuming a target enters the tracking area from point 0 for  $L$  meters as shown in Figure 2(a), we first derive  $P_r$ , the probability that a single sentry node detects this target. Obviously, the nodes that may detect the target must be in the rectangle or the semi-circle shown in the Figure 2(a). The size of the area is  $2SR \cdot L + \pi \cdot SR^2/2$ , where  $SR$  is the Sensing Range. For a single node located at  $(x, y)$  in this area, the probability that the node detects the target  $P(x, y)$  is  $SDC + l(x, y)/(P \cdot TS)$ , where  $l(x, y)$  is the overlapping length of the node's sensing range and the target's trace, and  $TS$  is the Target Speed. If we consider all possible locations in this area, we can get  $P_r$  in Equation 1 by integrating and normalizing the  $P(x, y)$  over the area. We note that when  $x, y$  is in the circle (area A) as shown in Figure 2(b),  $l(x, y) = \sqrt{SR^2 - y^2} + L - x$ .

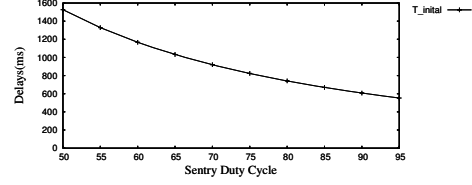


Figure 3: Initial Delay vs. SDC

When  $(x, y)$  is in area B,  $l(x, y) = 2\sqrt{SR^2 - y^2}$ .

$$P_r = \frac{\int_A (SDC + \frac{\sqrt{SR^2 - y^2} + L - x}{P \cdot TS}) ds + \int_B (SDC + \frac{2\sqrt{SR^2 - y^2}}{P \cdot TS}) ds}{(2SR \cdot L + \pi SR^2/2)} \quad (1)$$

$$= SDC + \frac{\pi \cdot SR \cdot L}{(2L + \pi \cdot SR/2) \cdot TS \cdot P}$$

We note that  $P_r$  calculated by Equation 1 is valid only when the target speed is faster than  $2SR/(P - P \cdot SDC)$ . We have also derived a slower-target case, which is of less interest to the real-time tracking. Therefore, we omit it here due to the space constraint, please refer [3] for more details.

Now we are ready to provide a statistical real-time guarantee for the initial activation process, i.e. we need to ensure a target is detected before the sub-deadline  $D_{initial}$ . Equivalently, a target should be detected before it enters for  $L = TS \cdot D_{initial}$  meters. Obviously,  $P(T_{initial} < D_{initial})$  equals  $P(T_{initial} \cdot TS < L)$ , where  $P(T_{initial} \cdot TS < L)$  is the probability that at least one of nodes in the area (A+B) detects the target. If there are  $n$  nodes in the area, the probability that at least one of them detects the target is  $1 - (1 - P_r)^n$ . Suppose the sentry density is  $D_s$  and  $n$  conforms to a Poisson distribution with parameter  $\lambda = (2SR \cdot L + \pi \cdot SR^2/2)D_s$ , therefore, the probability that the initial activation finishes before sub-deadline  $D_{initial}$  is:

$$P(T_{initial} < D_{initial}) = P(T_{initial} \cdot TS < L) = 1 - e^{-P_r \cdot \lambda} \quad (2)$$

Equation 2 identifies a feasible region for us to decide the system parameters such as sentry duty cycle (SDC) and sensing range (SR) to ensure the real-time property in Phase A. In addition, we can obtain the expected value of  $T_{initial}$  from the formula  $E(T_{initial}) = \int_0^\infty (1 - P(T_{initial} < t)) dt = \int_0^\infty (1 - P(SD < TS \cdot t)) dt$ . According to Equations 1 and 2, we have the expected delay for a fast target:

$$E(T_{initial}) = \frac{e^{-SDC \cdot \pi \cdot SR^2 \cdot D_s/2}}{(2SR \cdot SDC \cdot TS + \pi SR^2/P) D_s} \quad (3)$$

One caveat in the analysis needs some attention. Above we derive the expected detection delay for a duty cycle based system with *random deployment*. However, sentry nodes are located more evenly than totally randomly case [12]. Fortunately, we can prove that the random deployment case provides a theoretical upper bound for the sentry-based deployment case. It can be easily proved that if for all  $t$ ,  $P(T_1 < t) > P(T_2 < t)$ , we must have  $E(T_1) < E(T_2)$ . For  $0 < P_r < 1$ ,  $1 - (1 - P_r)^n$  is a

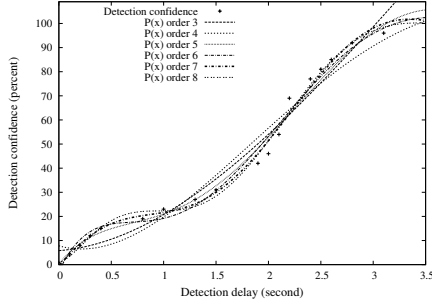


Figure 4: Detection Confidence vs. Detection Delay

strictly concave function of  $n$ . Therefore,  $E(1 - (1 - P_r)^n) \leq 1 - (1 - P_r)^{E(n)}$ , and the left side of the equation equals the right side if and only if  $n$  is a constant. Given the same  $E(n)$ , the more scattered the distribution of  $n$  is, the smaller the value of  $E(1 - (1 - P_r)^n)$  is. Since the sentry nodes are selected more uniformly than the random case,  $P(T_{initial} < D_{initial})$  for the sentry based system is greater than a totally randomly distributed system, and therefore the expected delay is smaller. The expected delay for the random case can be used as an upper bound for the expected detection delay for a more evenly distributed system. Later, we will see from the simulation that the analytical result overestimates the  $T_{initial}$  by 15%.

We can further take the detection delay  $T_{detection}$  into account, since a successful detection in Phase B activates a full tracking process. In this case, we establish an equivalent model for  $T_{initial}$ . Specifically, in Equation 3, we substitute  $SDC$  with the effective sentry duty cycle  $SDC_{eff} = SDC - T_{detection}/P$  and substitute  $SR$  with the effective sensing range  $SR_{eff} = \sqrt{SR^2 - (T_{detection} \cdot TS/2)^2}$ . Figure 3 gives a more concrete view of the tradeoff between  $SDC$  and expected  $T_{initial}$ . We take parameters from the real VigilNet implementation:  $D_S = 0.01 \text{ node/m}^2$ ,  $P = 10 \text{ s}$ ,  $SR = 10 \text{ m}$ ,  $TS = 10 \text{ m/s}$  and  $T_{detection} = 1000 \text{ ms}$ . This result is consistent with what we obtained from the real experiments and simulations.

## 4.2 Sentry Detection Delay and Its Tradeoffs

After the initial delay in Phase A, a target approaches the vicinity of a sensor, which begins to observe a different signal pattern than that without a target. With the current sensing algorithms, the signal pattern can be amplitude, frequency, or a combination of the two. We call the signal pattern corresponding to a target a *target signature*. The recognition of a target signature indicates a sensor-level detection, and produces data for higher-level detection and classification algorithms.

As defined before,  $T_{detection}$  is the time for a detection algorithm to recognize a target signature. This delay must be smaller than a certain sub-deadline  $D_{detection}$ . Multiple reasons contribute to this delay. First, the sensor hardware has a response delay for the physical signals that the target generates. Second, the sensing circuitry requires special operations with a further delay.

For example, the magnetometer in MICA2 node [5] takes about  $35 \text{ ms}$  to stabilize after the potentiometer adjustment. Third, the sampling is discrete and periodic, not continuous, which leads to sampling delay. Finally, the target signature itself may be time related (e.g., a certain frequency), which can not be recognized by just one sample.

Now we describe how to decide the sub-deadline  $D_{detection}$ . Obviously, a detection algorithm must finish before a target moves out of the sensing range of a node. Suppose that the nominal sensing area is a circle with a fix sensing range  $SR$ , the amount of time a target stays in a node's sensing range can be derived from the speed of the target,  $TS$ , and the minimum distance from the target's trajectory line to the sensor node. Since the target trajectory intersects with the sensing circle randomly, we assume this minimum distance is uniformly distributed within  $[0, R)$ , therefore the probability of a target stays in one sensing circle for at least  $D_{detection}$  seconds can be calculated as

$$P(t > D_{detection}) = \begin{cases} \sqrt{1 - \frac{(TS \cdot D_{detection})^2}{4SR^2}} & D_{detection} < \frac{2SR}{TS} \\ 0 & D_{detection} \geq \frac{2SR}{TS} \end{cases} \quad (4)$$

According Equation 4, the sub-deadline  $D_{detection}$  can be decided by choosing a desired  $P(t > D_{detection})$  value.

In addition, we desire to know how a detection algorithm performs under a given sub-deadline  $D_{detection}$ . We define the *Detection Confidence* (DC), as the confidence on the target detection, i.e. 100% DC indicates this sensor has no doubt about the existence of the target. Normally, the longer  $D_{detection}$  is, the more information about target signature a sensing algorithm can obtain, and therefore, it can achieve a higher detection confidence  $DC$ . Such relationship depends on the type of sensors. In order to quantitatively analyze the relation between  $DC$  and  $D_{detection}$  as a case study, we performed experiments on XSM motes with the magnetic sensing algorithm detecting a moving vehicle in an outdoor environment. We approximate the sensing range as 7 meters around the sensor node, according to empirical data. Figure 4 plots the relation between the detection confidence and the detection delay, based on the experiments. As we can see from the figure,  $DC$  does not have a linear relation to  $D_{detection}$ . Based on experimental measurements, we use a polynomial to characterize  $DC$  versus  $D_{detection}$ . Figure 4 shows a series of polynomials of different orders that fit the points representing the relation between the detection confidence and the detection delay. The plotting indicates that the polynomials of an order higher than 5 are fairly close to each other and fit the points well. Hence, we choose the polynomial of order 5 to characterize the relation, as shown below.

$$DC = f(D_{detection}) = \sum_{i=0}^5 a_i D_{detection}^i \quad (5)$$

The coefficients of the polynomial calculated from the curve fitting are  $a_5 = 1.0999$ ,  $a_4 = -13.1138$ ,  $a_3 = 51.3443$ ,  $a_2 = -73.2343$ ,  $a_1 = 54.6671$ ,  $a_0 = 0.2402$ . The polynomial

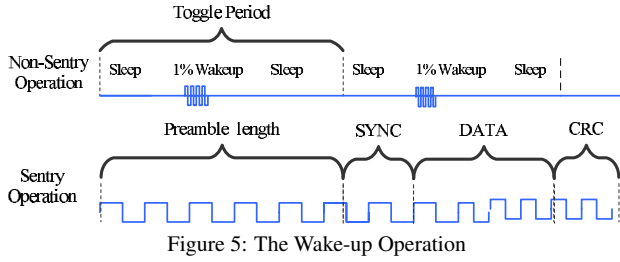


Figure 5: The Wake-up Operation

$f(D_{\text{detection}})$  characterizes the relation of the detection confidence and the imposed sub-deadline  $D_{\text{detection}}$  when the vehicle is moving at a relatively low speed. In the scenarios where the vehicles move faster, the detection delay tends to be shorter and the detection confidence will be higher because the targets impose a faster change to the sensor readings. Hence,  $f(D_{\text{detection}})$  represents a conservative estimation of the detection confidence, given a certain amount of time available to the sensor node to capture and process the target signals.

We note that in the analysis of the time-related properties of the sensing algorithms, we choose such a conservative-case approach instead of a worst-case approach. In many cases, the worst-case scenario is a rare event that the system is not designed to handle well. For example, with the magnetic sensing algorithm, the worst-case of detection delay is infinity – if a vehicle moves extremely slowly, it provides a low-frequency signal just as the back-ground noise, resulting in a non-detection for that target. We note that an analysis with such a worst-case scenario provides little insight into the system. To represent a reasonably practical scenario, we study a conservative case in which a target can be detected.

In conclusion, according to Equation 4 and 5, running a detection algorithm with a sub-deadline  $D_{\text{detection}}$ , one node can detect  $P(t > D_{\text{detection}})$  percent of targets with  $DC$  percent of the confidence in detection. This analysis justifies the benefits of fast detection algorithms and the need for group aggregation to improve the detection confidence.

### 4.3 Wake-up Delay and Its Tradeoff

Once a target is detected in Phase B, we need more nodes to join in order to increase the confidence in detection. We design a wake-up service to activate the non-sentry nodes after the sentry nodes detect the incoming targets. Different target speeds impose different sub-deadlines  $D_{\text{wake-up}}$  to the wake-up services.

Normally the wake-up service can be supported either through hardware or software. Several hardware solutions have been proposed in [6, 9]. Since the wake-up circuits accumulate the ambient energy slowly, the current hardware solutions are not fast enough for the real-time target tracking. Therefore, we propose a software-based wake-up strategy, which has a short

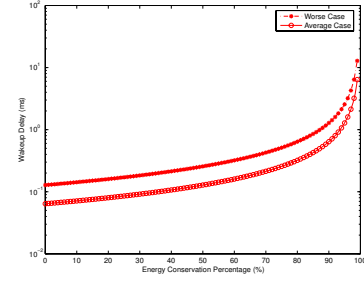


Figure 6: Wakeup Delay Vs. Non-Sentry Energy Saving

average delay and a predictable worse-case delay. The wake-up operation goes as shown in Figure 5. A non-sentry actually does not sleep all the time. It periodically wakes itself up, quickly senses the radio activity at a particular frequency. If no radio activity is detected, this node goes back to sleep, otherwise it remains active and starts to sample the environment. We control the non-sentry operation through two parameters: *Toggle Period (TP)* and *Channel Clear Access duration (CCA)*. The toggle period is defined as the time interval between two consecutive wake-up instances. The *CCA* is defined as the minimal time for a radio module to detect the existence of the radio signal. For example, the CC1000 radio transceiver takes at least 2ms (8 symbol periods, as specified by 802.15.4 [16]) to access the radio activity. Based on *TP* and *CCA*, we can get the Non-Sentry Duty Cycle (*NSDC*) as  $\frac{CCA}{TP}$ . At the sentry side, once a sentry detects a target, it broadcasts a radio message with a long preamble. This long preamble is guaranteed to be sensed by neighboring non-sentry nodes as long as this preamble has a length equal or longer than the toggle period of non-sentry nodes. The worst-case wake-up delay  $WC_{\text{Delay}}$  equals *TP*. In another word, the sub-deadline  $D_{\text{wake-up}}$  can be ensured trivially in our design by setting  $TP = D_{\text{wake-up}}$ . Let the power consumption for an active node during a unit of time be  $E$ , the energy consumption for a non-sentry node is  $\frac{E \times CCA}{TP}$ . Since the amount of time to check the radio activity (*CCA*) is constant for a specific radio hardware, the length of the toggle period determines the energy consumption rate in non-sentry nodes. In general, a long toggle period *TP* leads to a low energy consumption, however also leads to a long delay in waking up the non-sentry nodes. Figure 6 shows such a tradeoff, using the CC1000 radio transceiver for MICA2/XSM motes as an example. As shown in Figure 6, a sub-deadline of 200ms lead to a 99% energy saving for the non-sentry nodes.

### 4.4 Aggregation Delay and Its Tradeoffs

Once all nodes near the target are awoken in Phase C, the group-based tracking begins. To avoid an excessive power consumption, instead of relaying every detection message back, VigilNet sends only aggregates to the base stations for further processing. Such online aggregation process is subject to a cer-

tain sub-deadline  $D_{aggregation}$  determined by the target speed and the node density.

Specifically, we organize nodes in the vicinity of a target into one group. We use semi-dynamic leader election [21] to minimize the delay. Nodes that detect the target become the group members, which, upon detection, immediately report their own locations and sensing data to a leader. The leader then averages the locations of members as the estimates of the target positions, and sends such estimates to a base station. To filter out the sporadic false alarms of individual nodes, we introduce a configurable parameter,  $DOA$  (Degree of Aggregation), which forces the leader to withhold reports to a base station until the number of received member reports reaches  $DOA$ . To achieve a high confidence in target detection, one should set a high  $DOA$  value (e.g., 4). On the other hand, a higher  $DOA$  value inevitably introduces a longer group aggregation delay since the leader waits longer to expect more member reports. This tradeoff allows us to choose appropriate  $DOA$  to meet the sub-deadline  $D_{aggregation}$ .

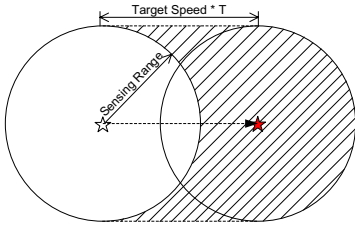


Figure 7: The Detection Areas Before and After Movement

The relation between  $DOA$  and the group aggregation delay is complicated by various factors, e.g., the sensing range, the target speed, and the node density. Therefore, we make several assumptions to simplify the analysis, including a circular sensing range, a straight target trajectory and randomly distributed nodes. Based on these assumptions, Figure 7 depicts the movement of a target with a speed  $TS$  for a time period  $T$ . Again, the sensing range of the target is  $SR$ . The white circle and the grey circle denote the detection area of the target before and after movement, respectively. Nodes located in the diagonally lined area are the new detectors of the target, which contribute to  $DOA$  by sending reports to the leader. To guarantee a certain sub-deadline  $D_{aggregation}$ , the number of new detectors must exceed or equal  $DOA$  before the sub-deadline  $D_{aggregation}$ :

$$D_{aggregation} \geq T_{aggregation} = \frac{DOA}{2 \cdot SR \cdot TS \cdot D} \quad (6)$$

where  $D$  represents the node density. Note that after the wake-up process, not only the sentry nodes but also the non-sentry nodes participate in the tracking. Equation 6 quantitatively reveals a feasible region for us to guarantee the sub-deadline  $D_{aggregation}$ . For example, if the network density ( $D$ ) and the sensing range ( $SR$ ) are fixed, we can exploit a feasible solution, using different  $DOA$  values under different target speeds. Figure 8 gives a more concrete design space by depicting the group

aggregation delay for varied  $DOA$  values and target speeds when the sensing range is 10m, the node density is 1 per 100  $m^2$ . We note that this result is consistent with the results obtained from large-scale simulation shown in Section 6.

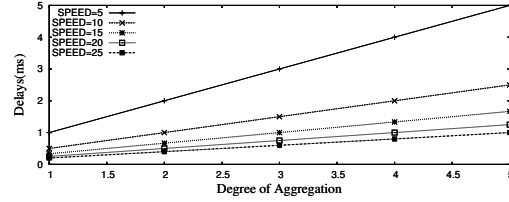


Figure 8: Minimal Group Aggregation Delay for Varying  $DOA$  and Target Speed

## 4.5 Communication Delay and Its Tradeoff

After group aggregation in Phase D, the leader delivers the aggregated tracking reports to a nearby base. Suppose the end-to-end communication sub-deadline is  $D_{e2e}$  and one-hop worst case communication delay is  $T_{WC\_MAC}$ , we need to ensure that the number of hops is smaller than  $D_{e2e}/T_{WC\_MAC}$ . For a given node density, the hop length  $L_{hop}$  can be estimated through Kleinrock-Silvester formula [19], which gives the correlation between the hop length  $L_{hop}$ , the communication range  $CR$  and the number of neighbors  $N$  as:

$$L_{hop} = CR \times \left(1 + e^{-N} - \int_{-1}^1 e^{-\frac{N}{\pi}(\arccos(t) - t\sqrt{1-t^2})} dt\right) \quad (7)$$

Therefore, to guarantee a sub-deadline  $D_{e2e}$ , when we deploy the network, we should ensure that every node can reach a base within a radius of  $L_{e2e}$ :

$$L_{e2e} = \frac{D_{e2e} \cdot L_{hop}}{T_{WC\_MAC}} \quad (8)$$

In VigilNet, the sub-deadline  $D_{e2e}$  is guaranteed by partitioning the whole network into multiple sections based on the Voronoi diagram [24]. Specifically, a network with  $n$  bases is partitioned into  $n$  Voronoi sections such that each section contains exactly one base and every node in that Voronoi section is closer to its base than to any other base inside the network.

## 4.6 Base Processing Delay and Its Tradeoffs

After a base receives the reports delivered in phase E, it performs the high-level processing such as the velocity estimation. In order to do so, a base node needs to accumulate several reports from the network. The delay to accumulate the reports  $T_{base}$  is subject to its sub-deadline  $D_{base}$ . We defined the minimal number of reports needed by the base as  $K$ . This value can be one, if the in-networking processing is sufficient. The frequency of

reports depends on the speed of the target and the aggregation of locations from nodes at different locations. From the analysis in the section 4, we know that after the target enters the system for time  $t$ , the expected number of nodes can sense the target is  $(\pi \cdot SR^2/2 + 2SR \cdot TS \cdot t)D$ . Obviously, if the target goes further for  $\Delta t$ , the expected number is increased by  $2SR \cdot TS \cdot \Delta t$ . Considering the detection delay  $T_{\text{detection}}$ , only nodes that are  $\sqrt{SR^2 - (T_{\text{detection}} \cdot TS/2)^2}$  meters away from the target trajectory can recognize the target. Therefore, we can estimate the number of report (NR) generated before the sub-deadline  $D_{\text{base}}$  as:

$$NR = (2TS \cdot D \cdot \sqrt{SR^2 - (T_{\text{detection}} \cdot TS/2)^2}) \cdot D_{\text{base}} \quad (9)$$

Alternatively, to guarantee  $D_{\text{base}}$ , we need to select the  $K$ , the minimal number of reports needed by the base, a value smaller than  $NR$ .

Now we consider how the selection of  $K$  impacts the accuracy in velocity estimation. Since each report only approximates the target location, there is an error in the result of velocity estimated using the least square method. Without loss of generality, we first consider the velocity along the x-axis. Statistics has established the variance of the estimated slope in a two-variable least square linear regression as

$$\frac{\sigma^2}{\sum_{i=1}^K (x_i - \bar{x})^2},$$

where  $\sigma$  is the standard deviation of the disturbance, which in our case is the detection error of a single report;  $x_i$  in our case is a timestamp. It is hard to get the distribution of  $\sum_{i=1}^K (x_i - \bar{x})^2$ , but a rough estimation can be obtained by a simplification so that the values of  $x_i$  are evenly distributed and  $x_i = i/(2D \cdot SR \cdot TS \cdot P_R)$ . Thus we can get an estimation of the standard deviation of the velocity:

$$\frac{4\sigma \cdot D \cdot SR \cdot TS \cdot P_R}{\sqrt{3K(K+1)(K-1)}}, \quad (10)$$

where  $\sigma$  is the standard deviation of the location error of a single report. Equation 10 reveals the tradeoff between the accuracy in tracking and the delay in base processing. In brief,  $T_{\text{base}}$  increases linearly with the number of reports required and the standard deviation of the velocity estimation reduces approximately linearly with  $K^{-3/2}$ .

#### 4.7 Summary of the Analysis and Tradeoffs

Dealing with the physical world, many sensor-based systems must respond to external stimuli within certain time constraints. Such constraints could change overtime with the changes of the application objectives. For example, a surveillance system should be able to track fast vehicles at a high-energy budget as well as slow personnel at a smaller budget. So it is desirable for a

system designer to have the ability to trade off the system parameters to satisfy certain real-time constraints. In this section, we use the deadline partition method to guarantee the sub-deadline of each phase, consequently guarantee the end-to-end deadline. This approach makes the real-time design for a complex sensor network manageable. Since VigilNet aims at various tracking scenarios, for a given end-to-end deadline, the actually partition among the phases would vary significantly. Our analysis is independent of how the sub-deadlines are assigned, which give the designer more flexibility to exploit the feasible regions until the end-to-end real-time requirement is met.

We note that this analysis can be generally applied to other tracking systems with or without certain features. For example, the tracking system presented in [2] does not consider the power management, which makes the analytical results of  $T_{\text{initial}}$  and  $T_{\text{wake-up}}$  trivially zero, while other analytical results are still applicable. We also note due to the unpredictable and statistical nature of environmental inputs (e.g., a target could move infinitely slowly), VigilNet is not quite amenable to the traditional worst-case real-time analysis. Nevertheless, the analytical results we provide can assist the designer to provide soft real-time guarantee and make guided decisions on the system configurations. In the next section, we validate our real-time design and analysis through a physical test-bed with 200 XSM motes as well as a large-scale simulator with 10,000 nodes.

## 5 Evaluation on Real System Performance

In the evaluation, we validate the analytical results as well as provide more insights on the timing issues from the real system and simulation perspectives.

### 5.1 System Configurations

A large portion of code of VigilNet is written in NesC [7], an modularized extension to the C programming language. Since the concept of traditional OS kernels does not exist in TinyOS [14], a NesC programmer can directly access the hardware devices including the sensors and flash memory, which facilitates the time analysis within a single node [23]. The network infrastructure in VigilNet is a multi-path diffusion tree rooted at bases. The contention-based B-MAC protocol [25] is the default media access control protocol, which has certain uncertainty in the communication delay. Three detection algorithms are designed separately for acoustic, magnetic and motion sensors. They identify the target signatures through a lightweight classification scheme as described in [8]. VigilNet consists 40,000 lines of code, supporting multiple existing mote platforms including MICA2, MICA2dot and XSM. The compiled image occupies 83,963 bytes of code memory and 3,586 bytes of data memory.

As a real-time online tracking system, VigilNet is designed to complete detection, classification and velocity estimation within 4 seconds. The field test was done on a T-shape dirt road in Florida as shown in Figure 9 from the aerial view. We deployed

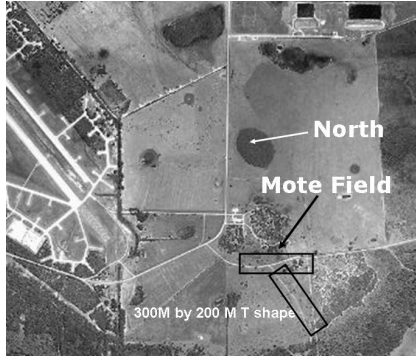


Figure 9: Deployment Site

200 XSM motes which are equipped with CC1000 radio, magnetic, acoustic, photo, temperature and passive infrared sensors (PIR). Along the road, nodes were randomly placed roughly 10 meters apart, covering one 300-meter road and one 200-meter road. Through localization [28, 10], nodes were aware of their positions. In order to measure various kinds of delay, all nodes within VigilNet synchronized with the base within 1~10 milliseconds using the techniques described in [22]. The time stamps of various actions such as initial detection were sent back to the base, so that we can calculate the delay. We used a Ford Explorer that weighted about 4000 lbs. as the target.

## 5.2 Delay Measurements

When a car enters the surveillance area at about 10 meters per second (22 mph), a detection report is issued first, followed by classification reports. Finally, after sufficient information is gathered, velocity reports are issued. Figure 10 illustrates the cumulative distribution of different delays. The communication delay (leftmost curve) is much smaller compared with other delays. About 80% of detections are done within 2 seconds. Over 80% of the classification and velocity estimations are made within 4 seconds. The empirical results from most runs are consistent with our analysis in Section 4 and the simulation results in Section 6.

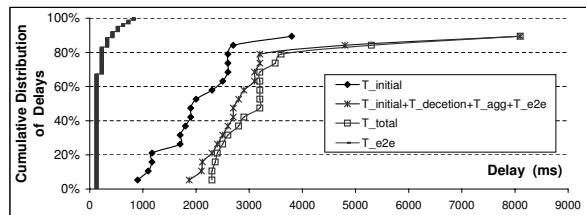


Figure 10: Various Delays Measurements from Field Test

We emphasize here that field experiments indicate that VigilNet meet its real-time requirement and our real-time analysis can approach the reality with a reasonable precision, despite the amount of complexity within the VigilNet (30 protocols inte-

grated). On the other hand, we acknowledge that due to various physical constraints, field experiments can only exploit a very limited design space and obtain a limited amount of data. Therefore, to understand the real-time properties in VigilNet at scale with a much large context, we provide a large-scale simulation in the next section.

## 6 Large-Scale Simulation

Our simulator emulates the tracking operations as shown in Figure 1. We distribute 10,000 nodes randomly within a 100,000  $m^2$  rectangle area. We run each experiment 30 times with different random numbers. The figures are plotted with the average value as well as the 95% confidence interval.

### 6.1 Experiment Setup

We note that our evaluation does not choose deadline/ sub-deadline miss ratios as the major metrics, because such an approach reveals less information about the tradeoff between actual delays and other system performance parameters. Since the mean value and 95% confidence intervals of the delays are plotted in the figures, one can determine the appropriate system settings for a given deadline requirement.

In our experiments, we study several system-wide parameters that directly affect the real-time properties of VigilNet. These parameters are: 1) the target speed (TS), 2) the physical delay in detection ( $T_{detection}$ ), 3) the sentry duty cycle (SDC), 4) the non-sentry duty cycle (NSDC), 5) the required degree of aggregation (DOA), 6) the sensing range (SR) and 7) the required number of reports for base processing (K). We match the simulations with the analysis to see how well they fit with each other.

We use the settings from the VigilNet system as the default values for these system parameters, which are listed in Table 1. Unless mentioned otherwise, the default values in Table 1 are used in all experiments. The metrics used to measure the system performance are mainly the six types of delays discussed in Section 2, the end-to-end delay and the energy consumption per day per node.

Table 1: Key System Parameters

Parameter	Definition	Default Value
<b>TS</b>	Target Speed	10 m/s
<b>SDC</b>	Sentry Duty Cycle	50%
<b>NSDC</b>	Non-Sentry Duty Cycle	1%
<b>DOA</b>	Degree of Aggregation	1%
<b>SR</b>	Sensing Range	10
<b>K</b>	Reports required by the base	1
<b>D</b>	Node Density	0.01 $m^{-2}$

### 6.2 Performance vs. Target Speed

The target speed determines the spatiotemporal distribution of events over a certain time period. It is crucial to understand



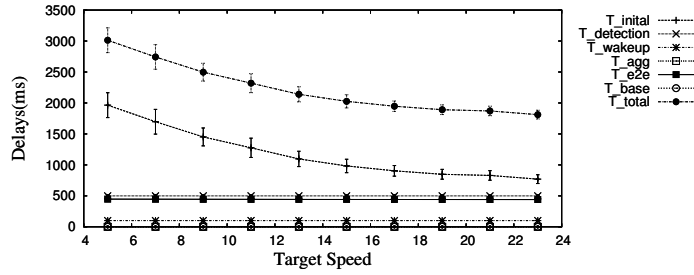


Figure 11: Delays vs. Target Speed

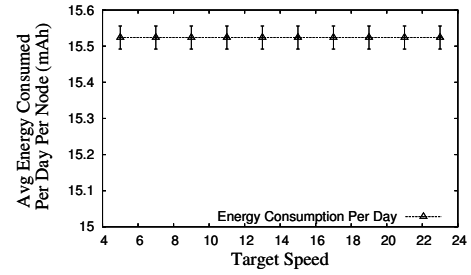


Figure 12: Energy Consumption vs. Target Speed

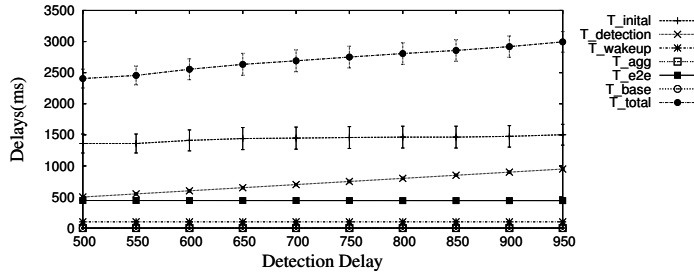


Figure 13: Delays under Varying Detection Delay

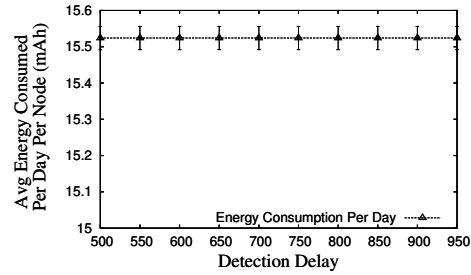


Figure 14: Energy Consumption vs. Detection Delay

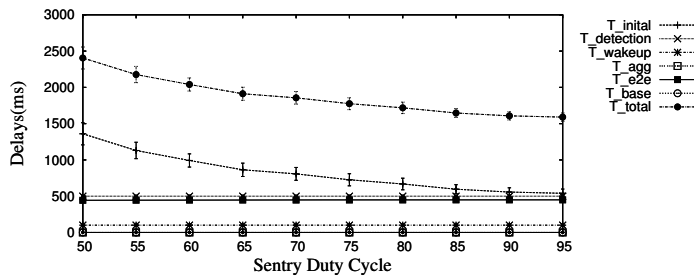


Figure 15: Delays vs. Sentry Duty Cycle

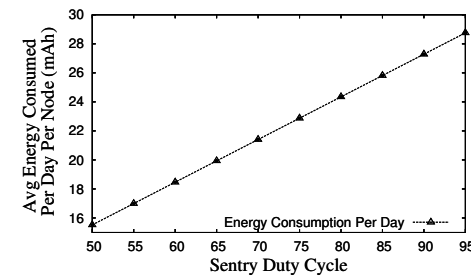


Figure 16: Energy Consumption vs. Sentry Duty Cycle

its impacts on the tracking performance. In this experiment, we incrementally increase the target speed (TS) from 5m/s to 15m/s in steps of 1 meter. As expected from our analysis in Section 4,  $T_{initial}$  and  $T_{aggregation}$  decrease with the target speed as shown in Figure 11. One interesting observation is that the descend rate of  $T_{initial}$  diminishes when  $TS$  becomes larger. This is because that a node needs a sufficient sensing time to ensure detection. It is possible that a quick target passes one sensor without detection, which negatively affects the  $T_{initial}$ . Since VigilNet deals with a rare event model, the energy consumed during the tracking is not perceptibly affected by the target speeds as shown in Figure 12.

### 6.3 Performance vs. Detection Delay

Different tracking systems use different sensing devices and detection algorithms, which have various detection delays  $T_{detection}$ . In this experiment, we increase the delay in the detection algorithm  $T_{detection}$  from 500 ms to 1000 ms in steps of 50 ms. It is interesting to observe in Figure 13 that at a speed of

10m/s, the detection delay has a small impact on the initial delay, however it contributes most significantly to the overall increase of the total tracking delay. Again, since the detection time is relatively small, this system parameter does not noticeably affect the overall energy consumption as shown in Figure 14.

### 6.4 Performance vs. Sentry Duty Cycle

From the analytical results in Section 4, we obtain an analytical delay curve between  $T_{initial}$  and  $SDC$  in Figure 3. In this experiment, we obtain another curves (Figure 15) through the simulation. By comparing these two results, we conclude that they are consistent with each other. For example, at a default 50% duty cycle,  $T_{initial}$  obtained from the analysis in Figure 3 is 1600ms, while  $T_{initial}$  obtained from the simulation (Figure 15) is 1360ms (Note that our analysis is relatively conservative). In addition, Figure 16 reveals that the energy consumption escalates linearly with the SDC, which indicates an efficient sentry scheduling algorithm is beneficial.

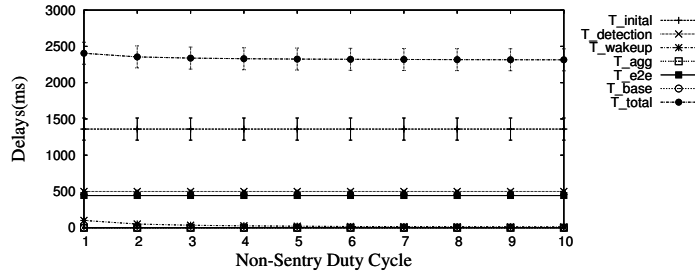


Figure 17: Delays vs. Non-Sentry Duty Cycle

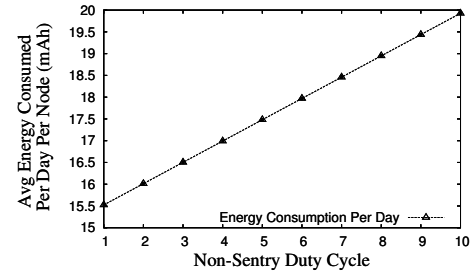


Figure 18: Energy Consumption vs. Non-Sentry Duty Cycle

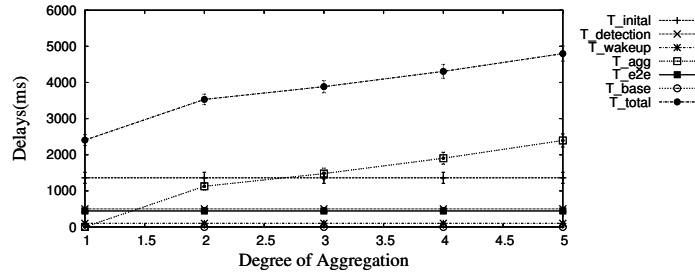


Figure 19: Delays vs. DOA

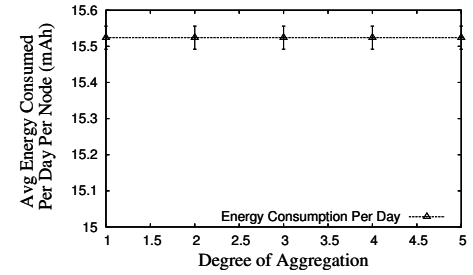


Figure 20: Energy Consumption vs. DOA

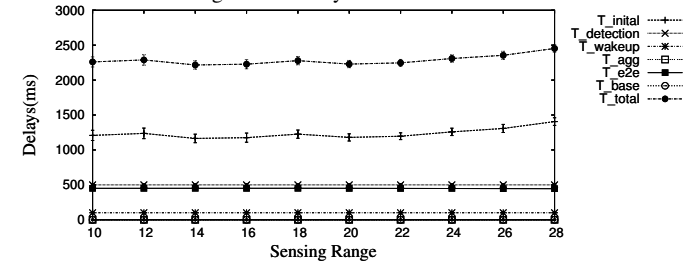


Figure 21: Delays vs. Sensing Range

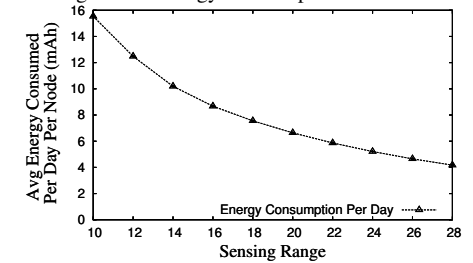


Figure 22: Energy Consumption vs. Sensing Range

## 6.5 Performance vs. Non-sentry Duty cycle

Here, we evaluate the impact of the wake-up operation on the delay and energy consumption. First, the simulation results confirm that the average wake-up delay is approximately half of the toggle period as predicted in Section 4.3. Since the wake-up delay  $T_{wakeup}$  is an order of magnitude smaller than other delays such as  $T_{initial}$ , a slight decrease in the wake-up delay shown in Figure 17 does not noticeably impact the overall delay. However, interestingly a slight increase of the Non-Sentry Duty Cycle leads to a significant increase of energy consumption as shown in Figure 18. This is because that the non-sentry nodes are by far the majority, so an duty-cycle increase of the non-sentry nodes leads to a quick increase in the total energy. This result indicates that it is beneficial to increase the wake-up delay, when possible, in exchange of the energy saving.

## 6.6 Performance vs. DOA

In-network processing through data aggregation can reduce the amount of data transmit over the network and increase the confidence in target detection. However to accumulate enough

report, it inevitably introduces a certain delay. This experiment studies the effects of data aggregation. We gradually increase the DOA threshold for a leader to report to base. Since the DOA value only affects the tracking phase, which has a small energy consumption, DOA's impact on the energy consumption is not noticeable. On the other hand, with a larger DOA value, it takes more time for a leader to collect the member reports. For example as shown in Figure 19, it takes as long as 2.39 seconds to achieve DOA value of 5. We note that this simulation result is again consistent with the analytical results shown in Figure 8, which has an estimated delay of 2.5 seconds.

## 6.7 Performance vs. Sensing Range

To accommodate various requirements in detection and classification, different tracking systems use sensors with different ranges. Figure 21 and Figure 22 investigate the impact of sensing range to the tracking performance and energy consumption. With a large sensing range, a smaller number of sentry is required. Therefore, the total energy consumption decreases quickly. For example in Figure 21, the energy reduces by 75%

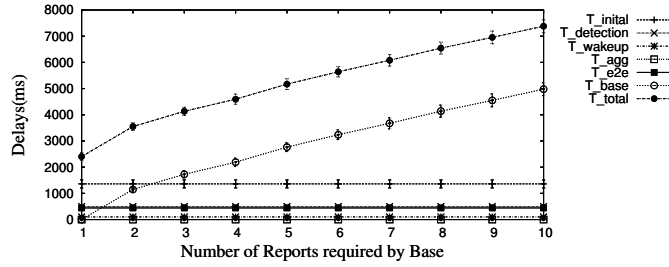


Figure 23: Delays vs. Num of Required Reports

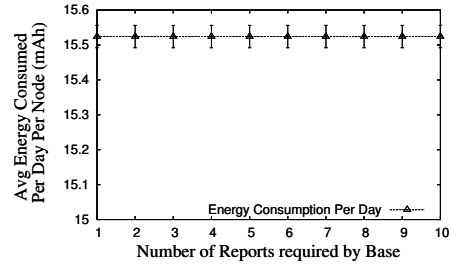


Figure 24: Energy Consumption vs. Num of Required Report

when the sensing range increases from 10m to 28m. It is interesting to see that the initial delay  $T_{initial}$  actually slightly increases. This is because the number of sentry nodes reduces while the coverage per sensor increases, the total coverage by all sentry nodes remains the same. We can derive from Equation 3 that expected  $T_{initial}$  is higher when the sensing range is smaller, given the same coverage in both cases. This analytic result is confirmed by the simulation results shown in the Figure 21. Due to the space constraint, we omit the detailed derivation here.

## 6.8 Performance vs. Number of Reports

To improve the estimation of target velocity and to classify targets with a high confidence, a base node normally needs to accumulate a certain number of spatiotemporal related reports from the same logic tracking group. This experiment investigates the impact of the number of reports required by a base to the tracking delays. Obviously, this only affects  $T_{base}$ . Figure 23 shows that  $T_{base}$  approximately increases linearly with the number of reports, which is expected by our analytical results in Section 4.6. Since the operation is done at the base, there is no energy impact to the sensor network as shown in Figure 24.

## 7 Related Work

Real-time protocols play an important role to guarantee the effectiveness of the interactions between wireless sensor networks and the physical world. RAP [20] uses a novel velocity monotonic scheduling to prioritize the real-time traffic and enforce such prioritization through a differentiated MAC Layer. Woo and Culler [31] propose an adaptive rate control scheme to achieve fairness among the nodes with different distances to a base station. Huang [15] et al. propose the Mobicast protocol to provide just-in-time information dissemination to nodes in a mobile delivery zone. Given the complete knowledge of traffic pattern, Li [18] proposes a SLF message scheduling algorithm to exploit spatial channel reuse, so that deadline misses can be reduced. The Lightning protocol [30] localizes the acoustic source with a bounded delay regardless of the node density. Carley [4] designs a periodic message scheduler to provide a contention-free predictable medium access control. Somasundara [27] proposes a mobile agent scheduling algorithm to col-

lect the buffered sensor data, before the buffer overflow occurs at the sensor nodes.

Besides the real-time protocol design, several research focuses on the time analysis for sensor networks. In [23], Mohan et al. provides a cycle-accurate WCET analysis tool for the applications running on the Atmega Processor Family. Abdelzaher [1] derives a real-time capacity bound for multi-hop wireless sensor networks. It is a sufficient schedulability condition for a class of fixed priority packet scheduling algorithms. Using this bound, one can determine whether a certain traffic pattern can meet its real-time requirement before hand.

With advances in the sensor techniques, several large-scale sensor systems have been built recently. The GDI Project [29] provides an environmental monitoring system to record animal behaviors for a long period of time. The shooter localization system [26] collects the time-stamps of the acoustic detection from different nodes within the network to localize the positions of the snipers. These systems mention some timing issues, however they do not treat real-time as a major concern. Our previous publications on VigilNet [12, 11] focus on the middleware services and overarching system integration. To the best of our knowledge, this work is the first to analyze the real-time performance and its tradeoffs in a real-world large-scale wireless sensor system.

## 8 Conclusion

In this paper, we demonstrate the feasibility to design a complex real-time sensor network, using the deadline partition method, which guarantees an end-to-end tracking deadline by satisfying a set of sub-deadlines. We also analytically identify the tradeoffs among system properties while meeting the real-time requirements. We validate our design and analysis through both a large-scale simulation with 10,000 nodes as well as a field test with 200 XSM nodes. We contribute a set of tradeoffs that are useful for the future development of real-time sensor systems. Given real-time constraints, a system designer can make guided engineering judgements on the system parameters such as the network density, the appropriate detection algorithm and the duty-cycle settings for the sensor nodes.

Finally, we acknowledge that although it is amenable to provide the worst-case real-time analysis for a certain protocol such

as the wake-up protocol in Section 4.3. However, due to the dynamic and unpredictable nature of the sensor networks, it is a long-term research goal for us to achieve precise worst-case real-time analysis across the whole system.

## Acknowledgements

This work was supported in part by the DAPRPA IXO offices under the NEST project (grant number F336615-01-C-1905), the MURI award N00014-01-1-0576 from ONR and NSF grant CCR-0098269. The authors specially thank the NEST program manager Vijay Raghavan for his valuable contributions.

## References

- [1] T. F. Abdelzaher, S. Prabh, and R. Kiran. On Real-Time Capacity Limits of Multihop Wireless Sensor Networks. In *IEEE RTSS*, 2004.
- [2] A. Arora, P. Dutta, S. Bapat, V. Kulathumani, H. Zhang, V. Naik, V. Mittal, H. Cao, M. Demirbas, M. Gouda, Y. Choi, T. Herman, S. Kulkarni, U. Arumugam, M. Nesterenko, A. Vora, and M. Miyashita. A Wireless Sensor Network for Target Detection, Classification, and Tracking. *Computer Networks (Elsevier)*, 2004.
- [3] Q. Cao, T. Yan, T. Abdelzaher, and J. Stankovic. Analysis of target detection performance for wireless sensor networks. In *DCOSS'05*, 2005.
- [4] T. W. Carley, M. A. Ba, R. Barua, and D. B. Stewart. Contention-free periodic message scheduler medium access control in wireless sensor/actuator networks. In *IEEE RTSS*, 2003.
- [5] CrossBow. *Mica2 data sheet*, 2003. Available at <http://www.xbow.com>.
- [6] P. Dutta, M. Grimmer, A. Arora, S. Biby, and D. Culler. Design of a Wireless Sensor Network Platform for Detecting Rare, Random, and Ephemeral Events. In *IPSN'05*, 2005.
- [7] D. Gay, P. Levis, R. von Behren, M. Welsh, E. Brewer, and D. Culler. The nesC Language: A Holistic Approach to Networked Embedded Systems. In *Proceedings of Programming Language Design and Implementation (PLDI) 2003*, 2000.
- [8] L. Gu, D. Jia, P. Vicaire, T. Yan, L. Luo, A. Tirumala, Q. Cao, J. A. S. T. He, T. Abdelzaher, and B. Krogh. Lightweight Detection and Classification for Wireless Sensor Networks in Realistic Environments. In *SenSys'05*, 2005.
- [9] L. Gu and J. A. Stankovic. Radio-Triggered Wake-Up Capability for Sensor Networks. In *Proceedings of RTAS*, 2004.
- [10] T. He, C. Huang, B. M. Blum, J. A. Stankovic, and T. Abdelzaher. Range-Free Localization Schemes in Large-Scale Sensor Networks. In *MOBICOM'03*, September 2003.
- [11] T. He, S. Krishnamurthy, L. Luo, T. Yan, R. Stoleru, G. Zhou, Q. Cao, P. Vicaire, J. A. Stankovic, T. F. Abdelzaher, J. Hui, and B. Krogh. VigilNet: An Integrated Sensor Network System for Energy-Efficient Surveillance. *ACM Transaction on Sensor Networks*, To appear.
- [12] T. He, S. Krishnamurthy, J. A. Stankovic, and T. Abdelzaher. An Energy-Efficient Surveillance System Using Wireless Sensor Networks. In *MobiSys'04*, June 2004.
- [13] T. He, P. Vicaire, T. Yan, Q. Cao, G. Zhou, L. Gu, L. Luo, R. Stoleru, J. A. Stankovic, and T. Abdelzaher. Achieving Long-Term Surveillance in VigilNet. In *IEEE Infocom*, 2006.
- [14] J. Hill, R. Szewczyk, A. Woo, S. Hollar, D. E. Culler, and K. S. J. Pister. System Architecture Directions for Networked Sensors. In *Proc. of Architectural Support for Programming Languages and Operating Systems (ASPLOS)*, pages 93–104, 2000.
- [15] Q. Huang, C. Lu, and G.-C. Roman. Spatiotemporal Multicast in Sensor Networks. In *SenSys 2003*, November 2003.
- [16] IEEE. IEEE Wireless Medium Access Control(MAC) and Physical Layer (PHY) Specifications for Low-Rate Wireless Personal Area Networks (LR-WPANs).
- [17] P. Juang, H. Oki, Y. Wang, M. Martonosi, L. Peh, and D. Rubenstein. Energy-Efficient Computing for Wildlife Tracking: Design Tradeoffs and Early Experiences with ZebraNet. In *Proc. of ASPLOS-X*, October 2002.
- [18] H. Li, P. Shenoy, and K. Ramamritham. Scheduling Messages with Deadlines in Multi-hop Real-time Sensor Networks. In *RTAS'05*, 2005.
- [19] L. Kleinrock and J. Slivester. Optimum transmission radii for packet radio networks or why six is a magic number. In *national Telecomm conference*, 1978.
- [20] C. Lu, B. M. Blum, T. F. Abdelzaher, J. A. Stankovic, and T. He. Rap: A real-time communication architecture for large-scale wireless sensor networks. In *IEEE RTAS*, 2002.
- [21] L. Luo, T. He, T. Abdelzaher, and J. Stankovic. Design and comparison of lightweight group management strategies in envirosuite. In *DCOSS '05: International Conference on Distributed Computing in Sensor Networks*, June 2005.
- [22] M. Maroti, B. Kusy, G. Simon, and A. Ledeczi. The Flooding Time Synchronization Protocol. In *SenSys'04*, pages 39–49, Nov. 2004.
- [23] S. Mohan, F. Mueller, D. Whalley, and C. Healy. Timing Analysis for Sensor Network Nodes of the Atmega Processor Family. In *IEEE RTSS*, 2004.
- [24] A. Okabe, B. Boots, K. Sugihara, and S. N. Chiu. *Spatial Tessellations: Concepts and Applications of Voronoi Diagrams*. Wiley, 2000.
- [25] J. Polastre and D. Culler. Versatile Low Power Media Access for Wireless Sensor Networks. In *Second ACM Conference on Embedded Networked Sensor Systems (SenSys 2004)*, November 2004.
- [26] G. Simon, M. Maroti, A. Ledeczi, G. Balogh, B. Kusy, A. Nadas, G. Pap, J. Sallai, and K. Frampton. Sensor Network-Based Countersniper System. In *SenSys'04*, November 2004.
- [27] A. A. Somasundara, A. Ramamoorthy, and M. B. Srivastava. Mobile Element Scheduling for Efficient Data Collection in Wireless Sensor Networks with Dynamic Deadlines. In *IEEE RTSS*, 2004.
- [28] R. Stoleru, T. He, and J. A. Stankovic. Walking GPS: A Practical Solution for Localization in Manually Deployed Wireless Sensor Networks. In *EmNetS-I*, October 2004.
- [29] R. Szewczyk, A. Mainwaring, J. Anderson, and D. Culler. An Analysis of a Large Scale Habit Monitoring Application. In *SenSys'04*, 2004.
- [30] Q. Wang, R. Zheng, A. Tirumala, X. Liu, and L. Sha. Lightning: A Fast and Lightweight Acoustic Localization Protocol Using Low-End Wireless Micro-Sensors. In *IEEE RTSS*, 2004.
- [31] A. Woo and D. Culler. A Transmission Control Scheme for Media Access in Sensor Networks. In *Proc. of Mobile Computing and Networking (Mobicom)*, 2001.
- [32] N. Xu, S. Rangwala, K. K. Chintalapudi, D. Ganesan, A. Broad, R. Govindan, and D. Estrin. A Wireless Sensor Network for Structural Monitoring. In *SenSys 2004*, 2004.